Microstructure Phase Imaging at 9.4T of the Human Brain applying Stepwise Filtering of Background Fields

Johannes Lindemeyer[1], Ana-Maria Oros-Peusquens[1], and N.-Jon Shah[1,2]

[1]*Institute of Neuroscience and Medicine - 4, Forschungszentrum Jülich, Jülich, Germany,* [2]*Department of Neurology, Faculty of Medicine, JARA, RWTH Aachen University, Aachen, Germany*

Introduction: Phase imaging and the reconstruction of local magnetic susceptibility distributions have recently been shown to exhibit excellent contrast with regard to microscopic structures in the human brain (e.g. [1,2,3]). Despite the remarkable quality of phase contrast induced by local structures, its order of magnitude lies significantly below shifts induced by long range distortions, such as static magnetic field shifts or large scale susceptibility interfaces e.g. generated by air cavities. It is therefore crucial to efficiently remove these influences while preserving local contrast at the same time. Numerous approaches have been introduced regarding this matter, including high-pass filters (as applied in [4]), polynomial filters and filters utilising either dipole distributions [5] or the harmonic nature of these distortions [6] to compensate for the shifts. After the introduction of the SPHINX algorithm in 2009 [7], which performs an expansion of the field in spherical harmonics, recently, a stepwise background filtering algorithm was presented, addressing the different sources of distortions in sequential steps [8]. The filter chain appears to be robust and convenient in local contrast preservation and was further enhanced in its functionality. In this abstract an application of the algorithm on 9.4T high-resolution *post mortem* brain data is presented.

Materials and Methods: Experiments were performed on a female *post mortem* brain obtained from the brain donor programme of the University of Düsseldorf and scanned in a custom-made cylindrical plexiglass container filled with formalin. Measurement was performed on a 9.4T human MR scanner (Siemens Healthcare, Erlangen, Germany). A single-channel transmit and eight-channel receive coil was used. Nevertheless, since a convenient algorithm for the correct recombination of the phase information of all channels is still under development only a single channel was considered for analysis. A standard slab-selective 3D-GRE sequence was applied including the following parameters: TR = 63ms, TE = 16.38ms, α = 25°, 12 averages and a bandwidth of 40Hz/pixel. An image matrix of 480x512x160 (sagittal slicing) was acquired with 240µm isotropic resolution and covers parts of the central brain, the brain stem and the cerebellum. A region-of-interest (ROI) featuring sufficient sensitivity of the coil element was extracted for further analysis. The ROI phase images were unwrapped using prelude (FSL [9]).

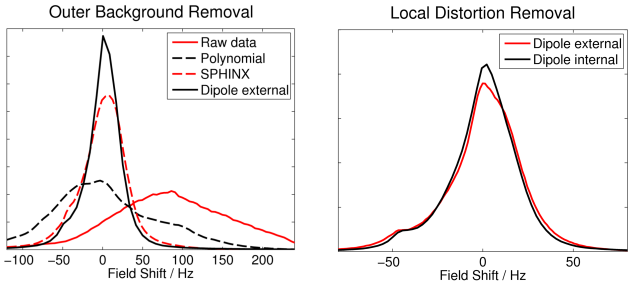

Fig. 1: Histograms of the phase distribution in different steps; the right plot shows the enhancement by local dipole correction

The complete background removal algorithm was implemented in Matlab® (The MathWorks Inc.). Initially a low-order, 3D-polynomial filter (utilising polyfitn [10]) is employed to remove dominant constant shifts and linear gradients to balance the phase distribution around zero. Higher order polynomials usually corrupt data integrity especially when susceptibility reconstruction is a sequential step. Harmonic fluctuations are thereafter addressed by the SPherical Harmonic INhomogeneity-suppresing eXpansion (SPHINX). It projects the measured phase or field map onto a basis of solid spherical harmonic functions which are orthonormal on the brain support – meaning on the ROI mask here. Spherical harmonics up to an order four were fitted in the presented example. Afterwards external sources of long- and short-range dipole fields are determined by a dipole continuum filter such as introduced by de Rochefort et al. [5]. The corresponding pseudo-susceptibility distribution outside the ROI is estimated by minimisation and the generated field is subtracted from the ROI after calculation. Remnant strong field variations that are unlikely to originate from brain tissue are occasionally generated by small cavities (in the case of *post mortem* brain also air bubbles) or erroneous phase/field values. These are taken into account by a local dipole filter, consisting of three substeps: thresholding identifies the affected voxels, local mask erosion connects neighboring voxels and finally another dipole continuum filter finds compensating fields for these areas. In the end, ideally, the remnant phase shifts will solely be generated by the susceptibility distribution inside the mask.

Results: The benefit of each background removal step is observable in the phase histograms plotted in Fig. 1. Apparently the phase distribution is steadily focused around zero throughout the different algorithm steps. The surface plots in Fig. 2 give a visual impression of the correction of the phase and also of the removal of strong local dipole-shaped fields induced by air bubbles inside the *post mortem* tissue (cerebellum). Fig. 3 shows the zoomed view of a representative slice from the background corrected phase volume. Several other exemplary applications of the stepwise filter algorithm show comparable results and good reliability.

Discussion and Perspective: The filter method presented here produces consistent phase or field maps and removes external and internal field influences originating either from static field impurities or susceptibility induced distortions. Low-pass or Gaussian filters have a comparable focusing effect on the phase distribution, but will at the same time destroy the phase integrity inside the mask. The outcome of the presented method is believed to embody an optimal basis for the reconstruction of local tissue susceptibility distributions, as corresponding studies in our Institute confirm. The filter chain is still under development and will offer a partly or fully automated algorithm for B_0 background field removal once. The cortical layers shown in Fig. 3 already give an impression of the potential use of such a filter for MR microscopy on phase data, albeit showing data from only one coil element.

References:

[1] Duyn, J. H., 2007, PNAS:104(28):11796-11801; [2] Deistung, A., 2008, MRM:60:1155-1168; [3] Langkammer, C., 2011, NeuroImage: doi:10.1016/j.neuroimage.2011.08.045; [4] Wharton, S., 2010, NeuroImage:53(2):515-25; [5] de Rochefort, L., 2010, MRM, 63:194–206; [6] Schweser, F., 2011, NeuroImage, 54:2789-2807; [7] Hirsch, S., 2009, High Field Systems & Applications, Poster 31; [8] Lindemeyer, J., 2011, ESMRMB, SoftDOI: 10.1007/s10334-011-0268-5, p. 507; [9] http://www.fmrib.ox.ac.uk/fsl/; [10] D'Errico, J., Copyright ©2007

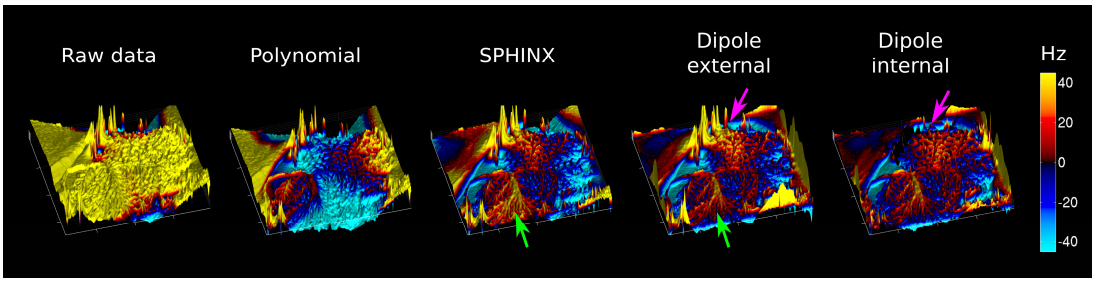

Fig. 2: Surface plots of the phase in different steps of the algorithm; the green arrows indicate corrected shifts from the external dipole distribution; magenta arrows show corrected local distortions, induced by air bubbles – the surroundings are affected by distortions originating in the thresholded voxels.

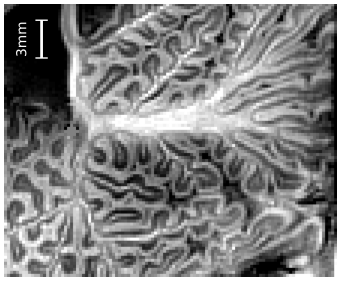

Fig. 3: Zoomed region, exhibiting structure of cerebellar cortical layers